THE JOURNAL OF PHYSICAL CHEMISTRY Letters

Letter

pubs.acs.org/JPCL

Ambipolar Charge Photogeneration and Transfer at GaAs/P3HT Heterointerfaces

Majid Panahandeh-Fard,[†] Jun Yin,[†] Michael Kurniawan,[†] Zilong Wang,[†,‡] Gle Leung,[†] Tze Chien Sum,[†] and Cesare Soci*[,†,‡]

[†]Division of Physics and Applied Physics, School of Physical and Mathematical Sciences and [‡]Centre for Disruptive Photonic Technologies, Nanyang Technological University, 21 Nanyang Link, Singapore 637371

Supporting Information

ABSTRACT: Recent work on hybrid photovoltaic systems based on conjugated polymers and III−V compound semiconductors with relatively high power conversion efficiency revived fundamental questions regarding the nature of charge separation and transfer at the interface between organic and inorganic semiconductors with different degrees of delocalization. In this work, we studied photoinduced charge generation and interfacial transfer dynamics in a prototypical photovoltaic *n*-type GaAs (111)B and poly(3-hexylthiophene) (P3HT) bilayer system. Ultrafast spectroscopy and density functional theory calculations indicate the coexistence of electron and hole transfer at the GaAs/P3HT interface, leading to the generation of long-lived species and photoinduced absorption upon creation of hybrid interfacial states. This opens up new avenues for the use of low-dimensional III−V compounds (e.g., nanowires or quantum dots) in hybrid organic/inorganic photovoltaics, where advanced bandgap and density of states engineering may also be exploited as design parameters.

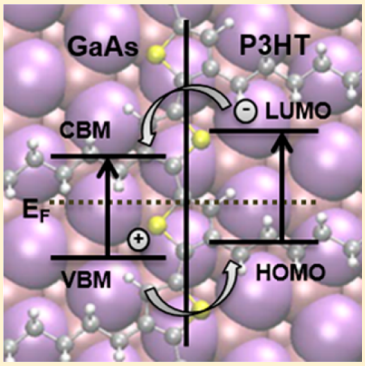

SECTION: Kinetics and Dynamics

Integration of conjugated polymers with inorganic nanocrystals such as nanowires, nanoribbons, and quantum dots, has proven an attractive strategy to increase power conversion efficiency (PCE) of organic photovoltaic (PV) devices.[1−7] Typically, in this type of hybrid solar cells, photogenerated excitons dissociate at the inorganic/polymer interfaces, transferring an electron to the semiconductor nanocrystals and leaving behind a positive polaron on the polymer chain. Charge carriers can then escape recombination and be extracted from opposite electrodes so that the competition between interfacial charge separation and charge recombination becomes the primary factor affecting the overall photocurrent.[8,9] One way to improve the PCE of polymer solar cells is to replace the commonly used fullerene-based acceptors with inorganic counterparts with higher electron mobility, such as group IV (Si[10] and Ge[11]), IV−VI (PbS[12] and PbSe[13,14]), II−VI (CdSe[15,16] and CdS[17]), or metal oxide (TiO_2[1] and ZnO[18,19]) compounds. So far, hybrid organic/inorganic PVs based on III−V semiconductors (e.g., GaAs and InP) and conjugated polymers demonstrated promising performance, thanks to the strong near-infrared absorption, the high carrier mobility, and the optimal staggered band alignment to common conducting polymers of III−V materials.[5,20−22] PCEs as high as ∼4.2% were obtained in GaAs/octithiophene bilayers,[23] ∼2.37% in GaAs nanowire/P3HT (poly(3-hexylthiophene-2,5-diyl)) bulk heterojunctions,[5] and ∼2.31% in GaAs/polymer bilayers.[24]

Despite the good characteristics of hybrid PVs, charge-transfer process at inorganic/polymer interfaces (e.g., GaAs/P3HT) is still not well understood.[25−28] Similarly, the fundamental nature of charged photoexcitations at the interface between highly delocalized inorganic naonocrystals and more localized, disordered conjugated systems is also of great fundamental interest but not completely unraveled.[29−33] Thus, better understanding of the nature of hybrid photoexcitation and their physical origin at III−V/polymer heterointerfaces is of primary importance and impact from both experimental and theoretical standpoints.

Few recent studies on charge transfer in hybrid III−V/organic semiconductor systems (small molecules, oligomers, and polymers) provided useful insights into interfacial processes upon photoexcitation as well as some guidelines for the design of efficient PV devices. Blackburn et al. investigated ultrafast hole-transfer from colloidal InP quantum dots to organic hole-transfer material by photoluminescence and transient absorption (TA) spectroscopy.[34] Lanzani et al. observed charge-transfer-induced exciton dissociation at the hybrid GaAs/oligothiophene bilayer interface. Subsequently, this group reported photoinduced electron transfer from $CuPcF_{16}$ to GaAs and from GaAs to C_{60} in hybrid $CuPcF_{16}$/GaAs[28] and C_{60}/GaAs[35] bilayer, respectively. Employing electric-field-induced second-harmonic generation, Zhu and coworkers reported photoinduced charge transfer from photoexcited GaAs to localized CuPc molecular orbital. This was attributed to charge-carrier separation in GaAs by the space-

Received: February 15, 2014
Accepted: March 18, 2014

   dx.doi.org/10.1021/jz500332z | *J. Phys. Chem. Lett.* 2014, 5, 1144−1150

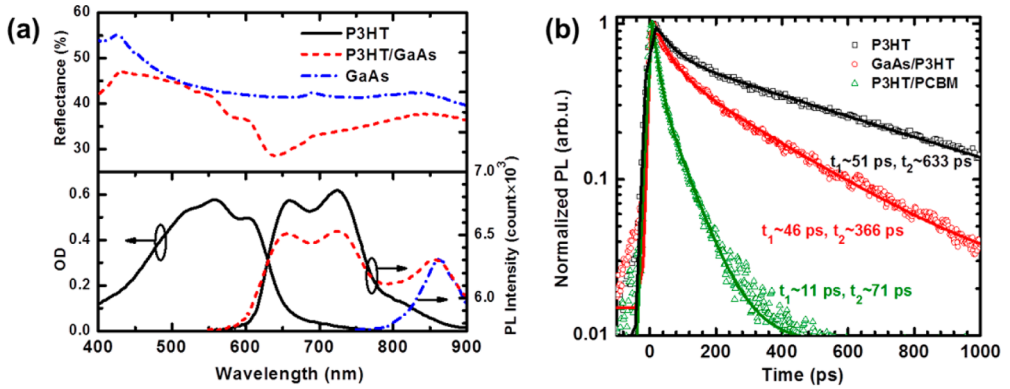

Figure 1. (a) Top panel: reflectance spectrum of GaAs (dashed-dotted line) and GaAs/P3HT (dashed line). Bottom panel: absorption and steady-state photoluminescence spectra of P3HT (solid lines), photoluminescence spectra of GaAs/P3HT bilayer (dashed line), and GaAs substrate (dashed-dotted line). (b) Time-resolved photoluminescence of pristine P3HT film (squares), P3HT/PCBM blend film (triangles), and GaAs/P3HT bilayer (circles). The time-resolved photoluminescence spectra were detected at 660 nm with photoexcitation at 500 nm. The photoluminescence decay dynamics were fitted to a bioexponential function (solid lines), where t_1 and t_2 are the extracted lifetimes. All films used for absorption and photoluminescence measurements were 40 nm thick.

charge field following ultrafast hole injection to CuPc.[26] More recently, Giustino and coworkers performed DFT modeling on a GaAs/polythiophene heterojunction, showing that the resulting interfacial dipole can lower the highest occupied molecular orbital (HOMO) of the conjugated polymer until the whole system attains equilibrium.[25] We have also considered the effect of surface polarity on the charge redistribution at GaAs/P3HT heterointerface by DFT modeling, showing that polar GaAs (111)B tends to facilitates hole transfer from the valence band (VB) states to the HOMO of P3HT, as compared with nanpolar surface GaAs (110).[36] While all of these studies demonstrated effectiveness of either electron or hole charge transfer at III−V/organic heterointerfaces, "ambipolar" charge transfer is expected to occur in GaAs/P3HT, whereby both electron transfer from the HOMO of P3HT to the conduction band (CB) of GaAs and hole transfer from excited states of GaAs to the LUMO of P3HT can occur simultaneously. This is an interesting new paradigm that may prove effective to improve charge photogeneration efficiency in hybrid PV devices.

We choose a prototype bilayer system based on a typical hole transporting material P3HT and *n*-type GaAs (111)B substrate. Our study focuses on the charge-carrier photogeneration and photoinduced interfacial charge transfer between GaAs and P3HT by combining various spectroscopy measurements and density functional theory (DFT) calculations. Photoluminescence and TA spectra with excitation energy above the P3HT optical gap clearly indicate that electron transfer takes place at GaAs/P3HT interface; this results in enhancement of polaron formation rate and increase in polaron lifetime. Moreover, energy-selective excitation below the optical gap of P3HT allows isolating a strong contribution of hole injection from GaAs to P3HT, a unique feature predicted by DFT modeling: for polar GaAs (111)B surfaces, calculations suggest that P3HT acts as an acceptor for hole transfer from the GaAs VB state to the HOMO of P3HT.[36] This shows that GaAs can perform a dual function of electron acceptor and light-harvesting material. Moreover, as its band energy diagram suggests, GaAs has one of the most favorable energetics for hole transfer to P3HT so that ambipolar charge transfer could indeed be achieved in GaAs/polymer solar cells with proper design engineering.

To fabricate GaAs/P3HT bilayer samples, we spun cast regioregular P3HT films at 1500 rpm on chemically etched, *n*-type (Si-doping~2×10^{18} cm^{-3}) GaAs (111)B substrates in an inert Ar atmosphere. The resulting P3HT film thickness, as measured by atomic force microscopy, was 40 nm. Figure 1a shows the reflectance spectra of a typical GaAs/P3HT bilayer, a bare GaAs reference substrate (top panel), and absorption spectrum of pristine P3HT film deposited on a quartz substrate (bottom panel). The GaAs substrate shows a broad reflectance band covering the entire visible region, while the absorption spectrum of pristine P3HT exhibits well-resolved, typical vibronic replicas at 610 (0−0), 555 (0−1), and 520 nm (0−2). The bottom panel of Figure 1a shows the corresponding steady-state photoluminescence spectra of P3HT, GaAs/P3HT bilayer, and bare GaAs. The GaAs/P3HT system shows main peaks originating from both P3HT, with emission peaks centered at 650 and 720 nm, and from the GaAs substrate, with an emission peak centered at ~860 nm. However, the intensity of photoluminescence transitions corresponding to P3HT is reduced in the bilayer compared with the pristine P3HT film with the same thickness. The quenching of steady-state photoluminescence of P3HT is a first indication of exciton population reduction upon charge-transfer across the heterointerface, similar to the well-known case of P3HT/PCBM blends, where radiative emission is completely quenched upon ultrafast (sub-50 fs) electron transfer to the fullerene acceptor.[37,38] Both emission and reflectance spectra of the GaAs/P3HT bilayer therefore suggest that GaAs acts as effective electron acceptor and light absorber in the combined hybrid system. Figure 1b shows a comparison between the photoluminescence transient dynamics of pristine P3HT, P3HT on GaAs, and a P3HT/PCBM bulk heterojunction (1:1 wt %). The photoluminescence lifetime of P3HT deposited on GaAs is found to be significantly reduced compared with the pristine P3HT sample, in agreement with the observed quenching of steady-state photoluminescence. Assuming that effective exciton dissociation takes place at the GaAs/P3HT interface, followed by photoinduced charge transfer between the two components, the charge-transfer efficiency can be estimated by comparing the exciton lifetimes extracted from Figure 1b.[37] The relative charge-transfer efficiency of the combined system, obtained from the ratio

dx.doi.org/10.1021/jz500332z | J. Phys. Chem. Lett. 2014, 5, 1144−1150

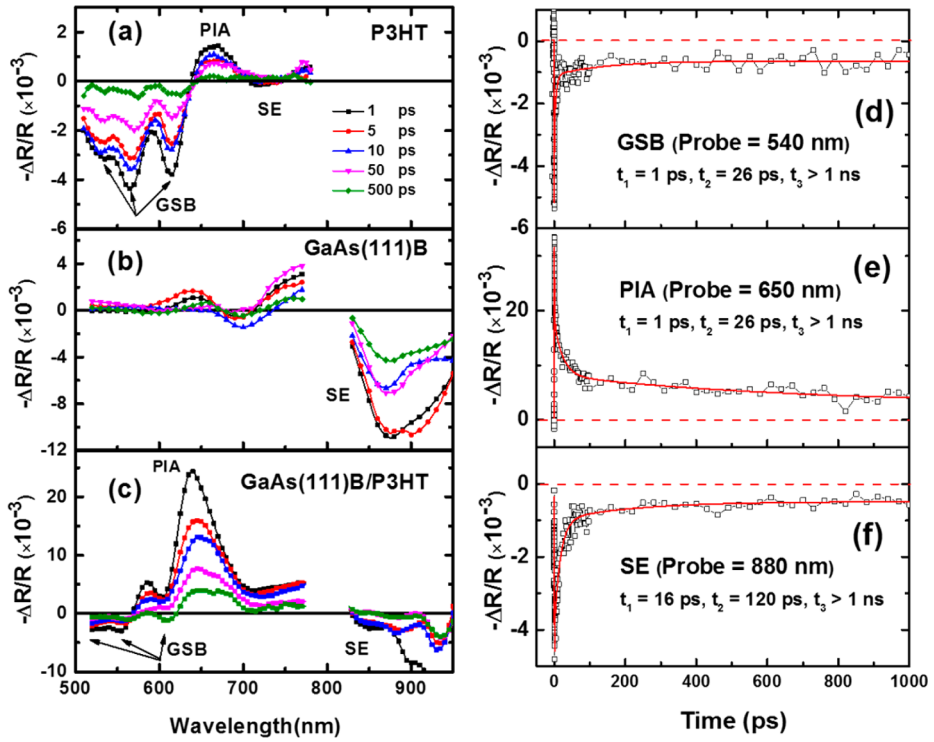

Figure 2. Left: transient reflectance spectra of pristine P3HT film (a), *n*-type GaAs (111)B (b), and hybrid *n*-type GaAs (111)B/P3HT bilayer (c) at different delay times following photoexcitation at 500 nm. Right: photoexcitation dynamics of the GaAs/P3HT bilayer at selected probe wavelengths: ground-state bleaching (GSB) probed at 540 nm (d); photoinduced absorption (PIA) probed at 650 nm (e); and stimulated emission (SE) probed at 880 nm (f). The solid lines are fitting of the data with multiexponential functions.

$k_{GaAs/P3HT}/k_{PCBM/P3HT}$, where $k_{GaAs/P3HT}$ is the fast component of the radiative decay of GaAs/P3HT and $k_{PCBM/P3HT}$ is that of the P3HT/PCBM blend (known to have charge transfer efficiency near 100%),[39] is on the order of 3%. This indicates that the GaAs/P3HT interface facilitates dissociation of photogenerated excitons, although charge-transfer efficiency is significantly lower than that in the P3HT/PCBM bulk heterojunction system, which offers larger interfacial area compared with the simple bilayer thanks to the interpenetrating morphology of the nanometer-scale donor−acceptor network. From the optimal type-II energy alignment of GaAs (111)B versus P3HT, electron transfer from P3HT to GaAs is indeed expected to yield positive polarons in P3HT; at the same time, hole injection from GaAs to P3HT is also anticipated to be energetically favorable (Figure S1 in the Supporting Information).[36]

Ultrafast time-resolved measurements (Figure 2) were performed to elucidate the interfacial charge-carrier dynamics at the hybrid GaAs/P3HT interface promptly after photoexcitation (t > 100 fs). Pump−probe spectroscopy was carried out with excitation wavelength of 500 nm and probe wavelengths in the range of 500−950 nm, collecting relative differential signals ($\Delta R/R$) in backscattering configuration. In GaAs/P3HT bilayers, the probe beam passes twice through the thin P3HT film after being reflected by the GaAs substrate. To mimic the effect of highly reflecting GaAs in control measurements of pristine P3HT, we spun cast films on quartz with a back aluminum metallization. Within this experimental configuration, the differential signal obtained by amplitude modulation of the pump beam effectively gauges the photoinduced TA of the P3HT film, together with photoinduced contributions from the interfacial layer. Negative signals correspond to an increase in the reflected probe light and originate from ground-state bleaching (GBS) or stimulated emission (SE), while positive signals are due to the decrease in reflected light intensity and originate from polaron absorption.

Figure 2a,b shows transient reflectance spectra of pristine P3HT film and *n*-type GaAs (111)B at different delay times. The spectra of P3HT (Figure 2a) exhibit negative features below 630 nm with three distinct vibronic peaks at 520 (0−2), 560 (0−1), and 610 nm (0−0) assigned to GSB, a very weak negative band between 700 and 750 nm arising from the SE of singlet excitons, and positive feature with a peak centered at 670 nm, which has been previously attributed to photoinduced absorption (PIA) of photogenerated charged species.[40,41] The spectra of *n*-type GaAs (Figure 2b) consist of three main features, two of which are PIA bands centered at 650 and 770 nm, and the third is a SE band centered at 875 nm. At early times after excitation, the SE band is broad due to hot-carrier cooling toward the band edge of GaAs.[33] Even at short times, the transient reflectance spectra of GaAs/P3HT bilayer (Figure 2c) are significantly different than those of control GaAs and P3HT samples. In the transient reflectance spectra of the GaAs/P3HT bilayer, there are three main features: a positive PIA band between 570 and 770 nm with peak centered at 650 nm, a negative photobleaching (PB) band at shorter wavelengths (<570 nm), and an SE band of GaAs at longer wavelengths (>770 nm). The negative PB band shows characteristic peaks at about 520 and 560 nm, which are attributed to the GSB of P3HT due to state-filling of the ground excitonic and polaronic states. Conversely, the 0−0 vibronic feature at 600 nm appears as a positive signal, most likely due to an offset due to the spectral overlap of the PB with the tail of the PIA. A new positive PIA band appears above 630

dx.doi.org/10.1021/jz500332z | J. Phys. Chem. Lett. 2014, 5, 1144−1150

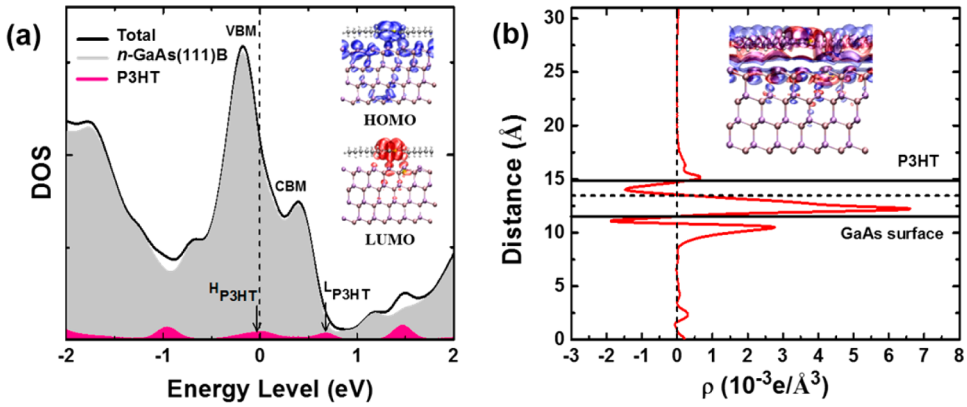

Figure 3. (a) Density of states and electronic orbital distribution of electronic orbitals of GaAs (111)B/P3HT hybrid system. The dashed line indicates the position of the Fermi energy. The insets show the electronic distribution of HOMO and LUMO of P3HT. (b) Charge redistribution in 1-D plane-averaged charge-density difference, $\Delta\rho(z)$, upon P3HT adsorption. The inset shows 3-D representation of the charge-density difference with an isovalue of ± 0.005 e/Å^3. The solid lines indicate the average positions of the GaAs surface and the P3HT plane, while the horizontal dashed line shows the interfacial distance at which charge depletion converts into charge accumulation.

nm with peak centered at 650 nm, which is quite long-lived and persists beyond the 500 ps temporal window of our measurements. Several factors may contribute to the observed long-lived PIA signal. According to the staggered band alignment of GaAs and P3HT, the GaAs/P3HT bilayer interface is expected to facilitate dissociation of photogenerated excitons. This results in the conversion of P3HT excitons into positive P3HT polarons, which is reflected in the transient reflectance signatures of the GaAs/P3HT bilayer. The appearance of strong PIA band could be due to the enhancement of polaron formation yield in P3HT as a result of charge-transfer-induced excitons dissociating at the hetero-interface: this would inhibit recombination of hole polarons in P3HT, thus increasing lifetime. The assignment of the PIA band to positive P3HT polarons is indeed supported by previous PIA and charge-modulation spectroscopy measurements performed on P3HT diodes.[42,43] In addition to the appearance of a strong PIA feature, the SE band of GaAs is featureless and broadened. Although SE of GaAs does not appear to be quenched at the initial time, consistent with steady-state PL data showing no reduction of GaAs emission in the bilayer and a previous report on GaAs nanowires embedded in P3HT,[25] SE is significantly reduced at later times, providing further evidence of ultrafast photoinduced charge transfer in this hybrid system. The second PIA band between 700 and 770 nm could result from the excitation of both GaAs and P3HT. We are not able to unambiguously assign this band to either PIA of P3HT species or GaAs because in this region the tail of PIA of P3HT is spectrally overlapped with the PIA of GaAs; therefore, we speculate that both GaAs and P3HT contribute to its formation. Transient reflectance measurements of intrinsic and p-type GaAs (111)B/P3HT bilayers also confirmed this assignment of PIA bands.

The dynamics of transient reflectance peaks in Figure 2d–f corresponding to PB (540 nm), PIA (650 nm), and SE (880 nm) confirms generation of long-lived species and PIA upon interfacial charge transfer across the heterointerface. In the GaAs/P3HT bilayer, dynamics of PB and PIA exhibit significantly longer lifetime of (>1 ns, ∼20% of the initial amplitude) in comparison with pristine P3HT film (Figure S2 and Figure S5 in the Supporting Information). Both the PB and the PIA dynamics rise nearly instantaneously (rise time is slightly longer than duration of pump–probe pulses). The rise time of PIA correlates well with the fast decay time of PB signal due to the depletion of the ground state (Figure S3 in Supporting Information). The appearance of longer lifetime PIA dynamics shows enhancement of polaron formation in P3HT due to the electron transfer to GaAs.[44] The prolonged PB dynamics also indicates small repopulation of excited states following charge transfer. Exciton dissociation and charge transfer across the GaAs/P3HT bilayer interface happen on a subpicosecond time scale.

DFT calculations were performed on the ground state of idealized Si-doped GaAs (111)B/P3HT bilayer model by replacing one As atom of GaAs top layer by Si atom. (See Figure S6 in the Supporting Information.) Charge transfer is usually determined by the electronic coupling strength, reorganization energy, energetics of the organic adsorbate and semiconductor, and density of states (DOS) of them. Figure 3a shows that the overall DOS of the GaAs and P3HT combined system (black lines) is largely dominated by the projected DOS of GaAs (shaded gray area), while the projected DOS of P3HT (blue line) only slightly perturbs the top of the VB of GaAs. States of the P3HT molecule extend over a broad energy range, and there is small overlap between the lowest unoccupied molecular orbital (LUMO) level or P3HT and the CB of GaAs compared with the relatively large overlap of the HOMO of P3HT and the GaAs VB. While the CB of GaAs gains overlap with the HOMO of P3HT, easing hole injection from GaAs to P3HT. The electronic charge rearrangement upon the formation of GaAs/P3HT interfaces is also shown in Figure 3b. The charge transferred from P3HT to the GaAs substrate was calculated as the difference $\Delta\rho(r) = \rho_{\mathrm{GaAs/P3HT}} - [\rho_{\mathrm{GaAs}} + \rho_{\mathrm{P3HT}}]$, where r is the position vector within the computational cell, ρ_{GaAs} is the charge density of the GaAs (111)B slab, ρ_{P3HT} is the charge density of P3HT layer without substrate, and $\rho_{\mathrm{GaAs/P3HT}}$ is the electronic charge density of the GaAs/P3HT interface. The in-plane average of $\Delta\rho$ along the z direction shown in Figures 3b provides quantitative estimate of electron ($\Delta\rho < 0$) and hole ($\Delta\rho > 0$) accumulation, indicating a large charge redistribution (up to $\sim 5.38 \times 10^3$ e/Å^3). Upon charge redistribution with adsorbed P3HT, the intrinsic surface dipole moment of GaAs surfaces is enhanced by induced charge displacement. To understand the origin of the interfacial dipole moment, we conducted a Löwdin charge analysis of the charge density for these hybrid systems.[45] By comparing the sum of

dx.doi.org/10.1021/jz500332z | J. Phys. Chem. Lett. 2014, 5, 1144–1150

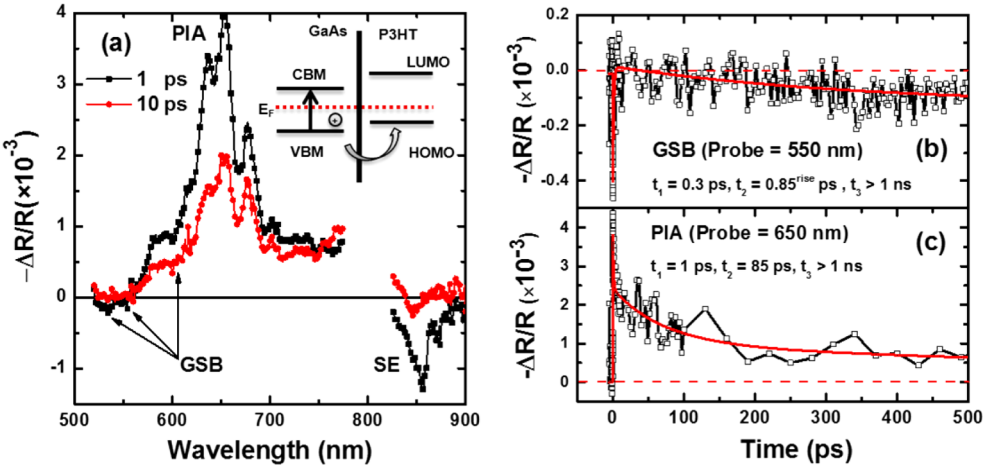

Figure 4. Transient reflectance spectra of GaAs/P3HT at 1 and 10 ps delay following energy-selective photoexcitation of GaAs at 800 nm (a). Transient reflectance decay profiles of photobleaching (PB) probed at 550 nm (b) and photoinduced absorption (PIA) probed at 650 nm (c). The solid lines are fitting of the data with multiexponential functions and the corresponding time constants are shown as insets.

the Löwdin charge on the GaAs and P3HT molecule before and after the formation of the interface, a total charge (ΔQ) of 0.223*e* for GaAs (111)B/P3HT is found to be transferred between P3HT and GaAs, which is slightly larger than the intrinsic GaAs (111)B/P3HT system (ΔQ = 0.209e), as shown in our previous work. This implies an efficient charge transfer compared with other hybrids systems, such as Cu (110)/petencene, ZnO/P3HT, ZnO/graphene, and so on.[36]

Ultrafast spectroscopy data and energy considerations suggest that the rapid generation of charges at the GaAs/P3HT heterointerfaces may be induced by either electron transfer from P3HT to GaAs or by hole injection from GaAs to P3HT. To address the nature of charge-transfer polarity, we lowered the excitation energy below the optical gap of P3HT (photoexcitation at 800 nm) to selectively excite GaAs and isolate the contribution of hole injection from GaAs to P3HT. As shown in Figure 4a, the transient reflectance spectra of hybrid GaAs/P3HT bilayer excited at 800 nm shows similar features as photoexcitation at 500 nm, namely, PB, PIA, and SE bands. Figure 4b,c shows dynamic profiles of PB and PIA probed at 550 and 650 nm. In this case, polaron-related bands are also rather long-lived. The main difference between dynamics of the different excitations (with energy above or below of the P3HT optical gap) appears in the characteristic PB signal below 560 nm. Promptly after excitation, the PB signal decays within 2 ps due to the predominant excitation of GaAs. After GaAs relaxation, the PB signal evolves and rises for a few picoseconds. Subsequently, the PB relaxes on a time scale much longer than our detection window of 500 ps.[27] The longer-lived charged polarons corresponding to the PB and the PIA signals are a clear indication of interfacial charge generation upon hole injection from GaAs (111)B to P3HT.[35] Therefore, when GaAs is selectively excited, holes are injected to P3HT; because the final state coincides with the electron-transfer state from P3HT to GaAs (111)B, this process gives rise to similar PIA signal. Similar results were also reported by Heeger and coworkers in PCPDBT/PCBM bulk heterojunction film, in which identical PB and PIA features of the polymer are observed with energy-selective excitation of PCBM. This was attributed to ultrafast hole transfer from the HOMO of PCBM to the higher HOMO energy of the of polymer, with identical final states following the electron transfer from PCPDBT to PCBM.[46]

In conclusion, we investigated charge photogeneration and transfer in a prototype hybrid GaAs/P3HT bilayer by combination of linear and ultrafast spectroscopy and DFT calculations. Data provide consistent evidence of ambipolar charge transfer of electrons and holes across the heterointerface, where large population of long-lived polarons is manifested by PIA and PB signatures with excitation either above or below the P3HT absorption energy. These findings are in agreement with DFT simulations that predict a fairly large interfacial dipole moment due to electrostatic interaction of electrons accumulated at the GaAs (111)B surface and holes below the P3HT molecule adsorbed at the surface. Ambipolar charge transfer can be regarded as an interesting new concept to optimize PV PCE of hybrid organic−inorganic devices. This work shows that efficient ambipolar transfer can be achieved at the interface between organic semiconductors and III−V compounds and may be further optimized by bandgap and DOS engineering. To increase charge separation and reduce recombination pathways, large interfacial areas in contact with the organic materials would be required in hybrid solar cells exploiting this concept, similar to bulk heterojunctions. This may be achieved using low-dimensional crystals, for instance, nanowires and quantum dots, as solution additives, while preserving conventional OPV fabrication techniques and architectures.

EXPERIMENTAL METHODS

Steady-state absorption and reflectance spectra were recorded by using a BRUKER VERTEX 80 V Fourier transform infrared (FTIR) spectrometer with reflectance accessory at the incident angle of 11°.

Steady-State and Time-Resolved Photoluminescence. An optical parametric amplifier (OPA) (Light Conversion TOPAS) was employed as the excitation source. TOPAS itself was pumped by a 1 kHz Coherent Legend apparatus(800 nm center wavelength, 100 fs pulse width, and 1 mJ/pulse power). Steady-state photoluminescence was measured using a CCD (Acton Princeton Instrument PIXIS 400) coupled to a monocromator (Acton Research Corporation SpectraPro 2500i). Time-resolved photoluminescence was measured by employing fast triggered streak camera (Optronis FTSU-1) coupled to a

dx.doi.org/10.1021/jz500332z | *J. Phys. Chem. Lett.* 2014, 5, 1144−1150

monochromator (Spectral Products RS-232) and a CCD (Pro Sensicam).

Transient Reflectance Spectroscopy. Transient reflectance data were collected with a femtosecond pump−probe setup in reflection geometry, where the excitation source was generated from the previously mentioned OPA. Pump−probe transient reflectance measurements were performed in the double-pass, back-scattering configuration in which light passes through the P3HT film and gets reflected off at the GaAs/P3HT interface, then collected and monitored using a monochromator/PMT configuration with lock-in detection. The pump beam was chopped at 83 Hz and referenced to the lock-in amplifier. The differential transient reflectance $\Delta R/R$ is defined as $((\Delta R/R) = ((R^{on}_{pump} - R^{off}_{pump})/R^{off}_{pump})$, where R^{on}_{pump} designates the probe reflected with pump on and R^{off}_{pump} designates the probe reflected with pump off. Second-order effects were minimized by using excitation density below 100 $\mu J/cm^2$ per pulse. The entire measurements were performed under vacuum (pressure $<10^{-3}$ Pa).

Density Functional Theory. The DFT with local density approximation (LDA) functional[47] calculations was carried out for studying interfacial structures and electronic properties using Quantum-ESPRESSO software package.[45] Ultrasoft (C, S, and H atoms) and norm-conserving of (Ga and As) atoms pseudopotentials were used to describe the electron−ion interactions. The electronic wave functions and charge density were expanded with an energy cutoff of 40 and 320 Ry, respectively. All surface and interface geometries were optimized with the direct energy minimization method of Broyden−Fletcher−Goldfarb−Shanno, until forces on all atoms became lower than 0.02 eV/Å and total energy difference between two optimization steps of the minimization procedures was less than 10^{-4} eV.

■ ASSOCIATED CONTENT

Ⓢ Supporting Information

Energy levels of GaAs/P3HT bilayer, PIA and GSB dynamics of pristine P3HT film, and GaAs/P3HT bilayer, laser intensity dependence of PIA of GaAs/P3HT, comparison of P3HT and GaAs/P3HT PIA decay dynamics, and doping effects in GaAs estimated by DFT. This material is available free of charge via the Internet at http://pubs.acs.org.

■ AUTHOR INFORMATION

Corresponding Author

*E-mail: csoci@ntu.edu.sg.

Notes

The authors declare no competing financial interest.

■ ACKNOWLEDGMENTS

We thank the xC-lab at NTU for ultrafast measurements and Prof. Guglielmo Lanzani and Dr. Dmitri Migas for fruitful discussions. Research was supported by Nanyang Technological University (grants M4080511 and M4080538) and by the Singapore Ministry of Education (project reference MOE2013-T2-044). M.P.-F. acknowledges financial support from a Yousef Jameel scholarship.

■ REFERENCES

(1) Huynh, W. U.; Dittmer, J. J.; Alivisatos, A. P. Hybrid Nanorod-Polymer Solar Cells. *Science* **2002**, *295*, 2425−2427.

(2) Law, M.; Greene, L. E.; Johnson, J. C.; Saykally, R.; Yang, P. Nanowire Dye-Sensitized Solar Cells. *Nat. Mater.* **2005**, *4*, 455−459.

(3) Liu, C. Y.; Holman, Z. C.; Kortshagen, U. R. Hybrid Solar Cells from P3HT and Silicon Nanocrystals. *Nano Lett.* **2009**, *9*, 449−452.

(4) Oosterhout, S. D.; Wienk, M. M.; van Bavel, S. S.; Thiedmann, R.; Koster, L. J. A.; Gilot, J.; Loos, J.; Schmidt, V.; Janssen, R. A. The Effect of Three-Dimensional Morphology on the Efficiency of Hybrid Polymer Solar Cells. *Nat. Mater.* **2009**, *8*, 818−824.

(5) Ren, S. Q.; Zhao, N.; Crawford, S. C.; Tambe, M.; Bulovic, V.; Gradecak, S. Heterojunction Photovoltaics Using GaAs Nanowires and Conjugated Polymers. *Nano Lett.* **2011**, *11*, 408−413.

(6) Reiss, P.; Couderc, E.; De Girolamo, J.; Pron, A. Conjugated Polymers/Semiconductor Nanocrystals Hybrid Materials—Preparation, Electrical Transport Properties and Applications. *Nanoscale.* **2011**, *3*, 446−489.

(7) Ehrler, B.; Walker, B. J.; Böhm, M. L.; Wilson, M. W.; Vaynzof, Y.; Friend, R. H.; Greenham, N. C. In Situ Measurement of Exciton Energy in Hybrid Singlet-Fission Solar Cells. *Nat. Commun.* **2012**, *3*, 1019.

(8) Zhou, Y.; Eck, M.; Krüger, M. Bulk-Heterojunction Hybrid Solar Cells Based on Colloidal Nanocrystals and Conjugated Polymers. *Energy Environ. Sci.* **2010**, *3*, 1851−1864.

(9) Kippelen, B.; Brédas, J.-L. Organic Photovoltaics. *Energy Environ. Sci.* **2009**, *2*, 251−261.

(10) He, L. N.; Lai, D.; Wang, H.; Jiang, C. Y.; Rusli. High-Efficiency Si/Polymer Hybrid Solar Cells Based on Synergistic Surface Texturing of Si Nanowires on Pyramids. *Small* **2012**, *8*, 1664−1668.

(11) Du Pasquier, A.; Mastrogiovanni, D. D. T.; Klein, L. A.; Wang, T.; Garfunkel, E. Photoinduced Charge Transfer Between Poly(3-hexylthiophene) and Germanium Nanowires. *Appl. Phys. Lett.* **2007**, *91*, 183501.

(12) Gunes, S.; Fritz, K. P.; Neugebauer, H.; Sariciftci, N. S.; Kumar, S.; Scholes, G. D. Hybrid Solar Cells Using PbS Nanoparticles. *Sol. Energy Mater. Sol. Cells* **2007**, *91*, 420−423.

(13) Cui, D.; Xu, J.; Zhu, T.; Paradee, G.; Ashok, S.; Gerhold, M. Harvest of Near Infrared Light in PbSe Nanocrystal-Polymer Hybrid Photovoltaic Cells. *Appl. Phys. Lett.* **2006**, *88*, 183111-1−183111-3.

(14) Semonin, O. E.; Luther, J. M.; Choi, S.; Chen, H.-Y.; Gao, J.; Nozik, A. J.; Beard, M. C. Peak External Photocurrent Quantum Efficiency Exceeding 100% via MEG in a Quantum Dot Solar Cell. *Science* **2011**, *334*, 1530−1533.

(15) Zhou, Y.; Riehle, F. S.; Yuan, Y.; Schleiermacher, H.-F.; Niggemann, M.; Urban, G. A.; Kruger, M. Improved Efficiency of Hybrid Solar Cells Based on Non-Ligand-Exchanged CdSe Quantum Dots and Poly (3-hexylthiophene). *Appl. Phys. Lett.* **2010**, *96*, 013304-1−013304-3.

(16) Grancini, G.; Biasiucci, M.; Mastria, R.; Scotognella, F.; Tassone, F.; Polli, D.; Gigli, G.; Lanzani, G. Dynamic Microscopy Study of Ultrafast Charge Transfer in a Hybrid P3HT/Hyperbranched CdSe Nanoparticle Blend for Photovoltaics. *J. Phys. Chem. Lett.* **2012**, *3*, 517−523.

(17) Ren, S.; Chang, L.-Y.; Lim, S.-K.; Zhao, J.; Smith, M.; Zhao, N.; Bulovic, V.; Bawendi, M.; Gradecak, S. Inorganic−Organic Hybrid Solar Cell: Bridging Quantum Dots to Conjugated Polymer Nanowires. *Nano Lett.* **2011**, *11*, 3998−4002.

(18) Beek, W. J. E.; Wienk, M. M.; Janssen, R. A. J. Hybrid Solar Cells from Regioregular Polythiophene and ZnO Nanoparticles. *Adv. Funct. Mater.* **2006**, *16*, 1112−1116.

(19) Oosterhout, S. D.; Wienk, M. M.; van Bavel, S. S.; Thiedmann, R.; Koster, L. J. A.; Gilot, J.; Loos, J.; Schmidt, V.; Janssen, R. A. J. The effect of Three-Dimensional Morphology on the Efficiency of Hybrid Polymer Solar Cells. *Nat. Mater.* **2009**, *8*, 818−824.

(20) Ong, P. L.; Levitsky, I. A. Organic/IV, III-V Semiconductor Hybrid Solar Cells. *Energies* **2010**, *3*, 313−334.

(21) Soci, C.; Bao, X. Y.; Aplin, D. P. R.; Wang, D. L. A Systematic Study on the Growth of GaAs Nanowires by Metal-Organic Chemical Vapor Deposition. *Nano Lett.* **2008**, *8*, 4275−4282.

(22) Sun, J. W.; Liu, C.; Yang, P. D. Surfactant-Free, Large-Scale, Solution-Liquid-Solid Growth of Gallium Phosphide Nanowires and Their Use for Visible-Light-Driven Hydrogen Production from Water Reduction. *J. Am. Chem. Soc.* **2011**, *133*, 19306−19309.

(23) Ackermann, J.; Videlot, C.; El Kassmi, A.; Guglielmetti, R.; Fages, F. Highly Efficient Hybrid Solar Cells Based on an Octithiophene−GaAs Heterojunction. *Adv. Funct. Mater.* **2005**, *15*, 810−817.
(24) Liang Yan, W. Y. Real Function of Semiconducting Polymer in GaAs/Polymer Planar Heterojunction Solar Cells. *ACS Nano* **2013**, *7*, 6619−6626.
(25) Yong, C. K.; Noori, K.; Gao, M.; Joyce, H. J.; Tan, H. H.; Jagadish, C.; Giustino, F.; Johnston, M. B.; Herz, L. M. Strong Carrier Lifetime Enhancement in GaAs Nanowires Coated with Semiconducting Polymer. *Nano Lett.* **2012**, *12*, 6293.
(26) Park, H.; Gutierrez, M.; Wu, X.; Kim, J. W.; Zhu, X. Optical Probe of Charge Separation at Organic/Inorganic Semiconductor Interfaces. *J. Phys. Chem. C.* **2013**, *117*, 10974.
(27) Cabanillas-Gonzalez, J.; Gambetta, A.; Zavelani-Rossi, M.; Lanzani, G. Kinetics of Interfacial Charges in Hybrid GaAs/Oligothiophene Semiconducting Heterojunctions. *Appl. Phys. Lett.* **2007**, *91*, 122113.
(28) Cabanillas-Gonzalez, J.; Egelhaaf, H.-J.; Brambilla, A.; Sessi, P.; Duò, L.; Finazzi, M.; Ciccacci, F.; Lanzani, G. Combined Spectroscopic Characterization of Electron Transfer at Hybrid CuPcF16/GaAs Semiconductor Interfaces. *Nanotechnology* **2008**, *19*, 424010.
(29) Bassani, F.; La Rocca, G. C.; Basko, D. M.; Agranovich, V. M. Excitons in Hybrid Organic-Inorganic Nanostructures. *Phys. Solid State.* **1999**, *41*, 701−703.
(30) Blumstengel, S.; Sadofev, S.; Xu, C.; Puls, J.; Henneberger, F. Converting Wannier into Frenkel Excitons in an Inorganic/Organic Hybrid Semiconductor Nanostructure. *Phys. Rev. Lett.* **2006**, *97*, 237401−237404.
(31) Zhang, Q.; Atay, T.; Tischler, J. R.; Bradley, M. S.; Bulovic, V.; Nurmikko, A. V. Highly Efficient Resonant Coupling of Optical Excitations in Hybrid Organic/Inorganic Semiconductor Nanostructures. *Nat. Nanotechnol.* **2007**, *2*, 555−559.
(32) Nizamoglu, S.; Sun, X. W.; Demir, H. V. Observation of Efficient Transfer from Mott-Wannier to Frenkel Excitons in a Hybrid Semiconductor Quantum Dot/Polymer Composite at Room Temperature. *Appl. Phys. Lett.* **2010**, *97*, 263106−263108.
(33) Yong, C. K.; Joyce, H. J.; Lloyd-Hughes, J.; Gao, Q.; Tan, H. H.; Jagadish, C.; Johnston, M. B.; Herz, L. M. Ultrafast Dynamics of Exciton Formation in Semiconductor Nanowires. *Small* **2012**, *8*, 1725−1731.
(34) Blackburn, J. L.; Selmarten, D. C.; Ellingson, R. J.; Jones, M.; Micic, O.; Nozik, A. J. Electron and Hole Transfer from Indium Phosphide Quantum Dots. *J. Phys. Chem. B.* **2005**, *109*, 2625−2631.
(35) Sessi, P.; Brambilla, A.; Finazzi, M.; Duò, L.; Cabanillas-Gonzalez, J.; Egelhaaf, H.; Lanzani, G.; Ciccacci, F. Evidence of Photoinduced Charge Transfer in C60/-GaAs(100) Bilayers by Pump−Probe Measurements. *Chem. Phys. Lett.* **2008**, *466*, 65−67.
(36) Yin, J.; Migas, D. B.; Panahandeh-Fard, M.; Chen, S.; Wang, Z. L.; Lova, P.; Soci, C. Charge Redistribution at GaAs/P3HT Heterointerfaces with Different Surface Polarity. *J. Phys. Chem. Lett.* **2013**, *4*, 3303−3309.
(37) Jarzab, D.; Szendrei, K.; Yarema, M.; Pichler, S.; Heiss, W.; Loi, M. A. Charge-Separation Dynamics in Inorganic-Organic Ternary Blends for Efficient Infrared Photodiodes. *Adv. Funct. Mater.* **2011**, *21*, 1988−1992.
(38) Piris, J.; Dykstra, T. E.; Bakulin, A. A.; van Loosdrecht, P. H. M.; Knulst, W.; Trinh, M. T.; Schins, J. M.; Siebbeles, L. D. A. Photogeneration and Ultrafast Dynamics of Excitons and Charges in P3HT/PCBM Blends. *J. Phys. Chem. C.* **2009**, *113*, 14500−14506.
(39) Guo, J. M.; Ohkita, H.; Benten, H.; Ito, S. Charge Generation and Recombination Dynamics in Poly(3-hexylthiophene)/Fullerene Blend Films with Different Regioregularities and Morphologies. *J. Am. Chem. Soc.* **2010**, *132*, 6154−6164.
(40) Mauer, R.; Howard, I. A.; Laquai, F. Effect of Nongeminate Recombination on Fill Factor in Polythiophene/Methanofullerene Organic Solar Cells. *J. Phys. Chem. Lett.* **2010**, *1*, 3500−3505.
(41) Jiang, X. M.; Osterbacka, R.; Korovyanko, O.; An, C. P.; Horovitz, B.; Janssen, R. A.; Vardeny, Z. V. Spectroscopic Studies of Photoexcitations in Regioregular and Regiorandom Polythiophene Films. *Adv. Funct. Mater.* **2002**, *12*, 587−597.
(42) Österbacka, R.; An, C.; Jiang, X.; Vardeny, Z. Two-Dimensional Electronic Excitations in Self-Assembled Conjugated Polymer Nanocrystals. *Science* **2000**, *287*, 839−842.
(43) Brown, P. J.; Sirringhaus, H.; Harrison, M.; Shkunov, M.; Friend, R. H. Optical Spectroscopy of Field-Induced Charge in Self-Organized High Mobility Poly (3-hexylthiophene). *Phys. Rev. B.* **2001**, *63*, 125204.
(44) Noone, K. M.; Subramaniyan, S.; Zhang, Q.; Cao, G.; Jenekhe, S. A.; Ginger, D. S. Photoinduced Charge Transfer and Polaron Dynamics in Polymer and Hybrid Photovoltaic Thin Films: Organic vs. Inorganic Acceptors. *J. Phys. Chem. C.* **2011**, *115*, 24403−24410.
(45) Giannozzi, P.; Baroni, S.; Bonini, N.; Calandra, M.; Car, R.; Cavazzoni, C.; Ceresoli, D.; Chiarotti, G. L.; Cococcioni, M.; Dabo, I. QUANTUM ESPRESSO: A Modular and Open-Source Software Project for Quantum Simulations of Materials. *J.Phys.: Condens. Matter* **2009**, *21*, 395502.
(46) Hwang, I.-W.; Cho, S.; Kim, J. Y.; Lee, K.; Coates, N. E.; Moses, D.; Heeger, A. J. Carrier Generation and Transport in Bulk Heterojunction Films Processed with 1, 8-octanedithiol as a Processing Additive. *J. Appl. Phys.* **2008**, *104*, 033706.
(47) Perdew, J. P.; Zunger, A. Self-Interaction Correction to Density-Functional Approximations for Many-Electron Systems. *Phys. Rev. B.* **1981**, *23*, 5048−5079.